

Polymerization Activators | Very Important Paper |

VIP Interaction of Neutral Donors with Methylaluminoxane

Harmen S. Zijlstra,<sup>[a]</sup> Anuj Joshi,<sup>[a]</sup> Mikko Linnolahti,<sup>[b]</sup> Scott Collins,<sup>[a]</sup> and J. Scott McIndoe\*<sup>[a]</sup>

**Abstract:** Methylaluminoxane (MAO) is a key activator for olefin polymerization catalysts, making its chemistry of ongoing interest. Strong and bidentate neutral donors such as 2,2'-bipyridine are effective abstractors of the dimethylaluminum cation,  $[\text{Me}_2\text{Al}]^+$ , from methylaluminoxane (MAO), while monodentate, weaker donors such as THF appear most prone to adduct formation with both free and bound trimethylaluminum. The ionization process can be readily investigated using electrospray

ionization mass spectrometry (ESI-MS) in fluorobenzene (PhF) solution. Complementary studies employing 1D and 2D  $^1\text{H}$  NMR spectroscopic studies in  $[\text{D}_5]$ bromobenzene solution provide details on the extent of ionization vs. donor-acceptor complex formation for the different donors studied. DFT studies employing different neutral model precursors and mono- vs. didentate donors shed light on possible mechanisms for ion-pair formation.

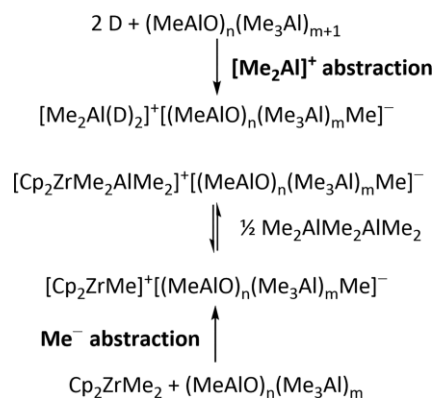
Introduction

Methylaluminoxane (MAO) is a widely used activator for the generation of molecular polymerization catalysts. It serves to scavenge impurities, while alkylating and activating suitable transition metal precursors.<sup>[1]</sup> The properties of MAO depend on the method of synthesis.<sup>[2,3]</sup> The efficacy of MAO as a co-catalyst or activator is dependent on the production of higher MW aluminoxanes, as lower MW materials such as  $\text{R}_2\text{AlOAlR}_2$  are largely ineffective as activators of single site catalysts.<sup>[2,3]</sup>

Measured properties of MAO, proportional to MW are time and temperature dependent, especially if stored at room temperature, where MAO undergoes aging and eventual gelation.<sup>[4]</sup> There is no direct method for measuring the MW of MAO aside from cryoscopic measurements, which are demanding in terms of both reproducibility and accuracy.<sup>[5a]</sup> Donor solvents such as 1,4-dioxane form donor-acceptor complexes with MAO of significantly lower MW than the native material by this technique.<sup>[5a]</sup> Neutral donors such as THF,<sup>[5b]</sup> pyridine<sup>[5b]</sup> or  $\text{Ph}_3\text{P}$ <sup>[5c]</sup> are often employed in order to determine the trimethylaluminum ( $\text{Me}_3\text{Al}$ ) content of MAO; the  $\text{Me}_3\text{Al}$  content of MAO has important consequences for catalyst activity.<sup>[6]</sup>

MAO is a strong Lewis acid, capable of reacting with transition metal carbon bonds via heterolytic cleavage leading to ion-pairs. In the case of a methyl group this is termed  $\text{Me}^-$  or methide abstraction (Scheme 1).<sup>[1]</sup> In the last few years, an alternate mechanism for ion-pair formation has been identified,<sup>[4b,7,8]</sup> with support from theoretical work.<sup>[9]</sup> This process

involves abstraction of  $[\text{Me}_2\text{Al}]^+$  from a neutral MAO precursor by a neutral donor,<sup>[4b,7,8]</sup> or a complex such as  $\text{Cp}_2\text{ZrMe}_2$ .<sup>[8,9]</sup> Note that the neutral MAO precursor in the case of  $[\text{Me}_2\text{Al}]^+$  abstraction has one more  $\text{Me}_3\text{Al}$  incorporated than does that for  $\text{Me}^-$  abstraction if the anion (or ion-pair) formed is to have the same formulae.



Scheme 1. Ionization mechanisms involving MAO.

The ion-pairs formed from MAO and various donors can be characterized by electrospray ionization mass spectrometry (ESI-MS) in fluorobenzene (PhF) solution.<sup>[8,10]</sup> We have shown a strong analogy between this technique and other methods such as NMR spectroscopy when it comes to activation of metallocene complexes.<sup>[11]</sup>

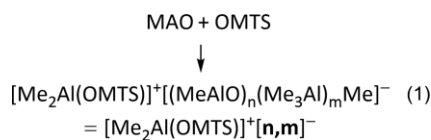
The reaction of the bidentate donor octamethyltrisiloxane (OMTS) with MAO leads to the ion pairs in Equation 1,<sup>[12]</sup> where a common cation  $[\text{Me}_2\text{Al}(\text{OMTS})]^+$  with  $m/z$  293 is partnered with MAO-based anions of the general formula shown.<sup>[8,10]</sup>

Since the anions  $[\mathbf{n}, \mathbf{m}]^-$  formed can be characterized in negative mode, this technique provides indirect information about the MAO-based, neutral oligomers (hereinafter  $\mathbf{n}, \mathbf{m}$ ) involved in forming ion-pairs. We have used this technique to study aging

[a] Department of Chemistry, University of Victoria, P. O. Box 3065 Victoria BC V8W3V6, Canada  
E-mail: mcindoe@uvic.ca  
<http://web.uvic.ca/~mcindoe/index.html>

[b] Department of Chemistry, University of Eastern Finland, P. O. Box 111, 80101 Joensuu, Finland

Supporting information and ORCID(s) from the author(s) for this article are available on the WWW under <https://doi.org/10.1002/ejic.201900153>.



of MAO at room temperature,<sup>[10]</sup> chlorination of MAO,<sup>[13]</sup> oxidation of MAO upon exposure to O<sub>2</sub>,<sup>[14]</sup> and modification of MAO by AlR<sub>3</sub>,<sup>[15]</sup> where the anion distribution changes in response to these processes.

In this paper we study the mechanisms for ion-pair formation, using a variety of neutral donors and ESI-MS and NMR methods with reference to theoretical models<sup>[16]</sup> for the anions and neutrals that are in the relevant size domain for MAO and the ion-pairs formed from it. The neutrals were located in a systematic grid search of the reactions of Me<sub>3</sub>Al with water,<sup>[16a,16b]</sup> while anionization by both [Me<sub>2</sub>Al]<sup>+</sup> abstraction and Me<sup>-</sup> abstraction involving MAO has been discussed in some detail previously.<sup>[9a,10]</sup>

## Results and Discussion

### Tetrahydrofuran

Tetrahydrofuran has long been recommended for the determination of Me<sub>3</sub>Al content of MAO using <sup>1</sup>H NMR spectroscopy. Typically, addition of 10 molar equivalents with respect to Al (4:1 v:v equiv. for 30 wt.-% MAO in toluene) has been recommended for this procedure; this leads to optimal separation of the sharp signal, due to Me<sub>3</sub>Al-THF, from the main MAO resonances (Figure 1).<sup>[5b]</sup>

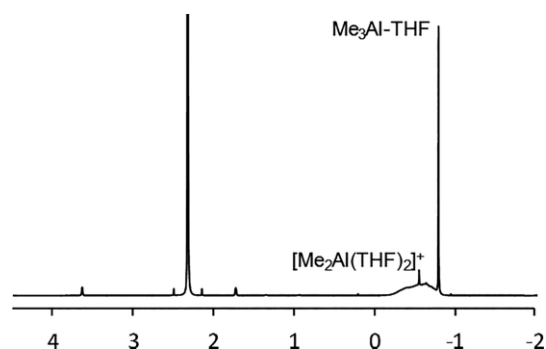


Figure 1. <sup>1</sup>H NMR spectrum of a sample of commercial MAO (30 wt.-% in toluene) containing 10 equiv. [D<sub>8</sub>]THF.

Though not recognized at the time of this first report, an additional sharp signal that is superimposed upon the main MAO resonance arises from the formation of [Me<sub>2</sub>Al(THF)<sub>2</sub>]<sup>+</sup>, as shown by comparison to authentic samples of this cation partnered with e.g. a [B(C<sub>6</sub>F<sub>5</sub>)<sub>4</sub>]<sup>-</sup> anion,<sup>[7]</sup> an assignment subsequently confirmed by Bochmann and co-workers.<sup>[4b]</sup>

Through baseline subtraction (or deconvolution<sup>[17]</sup>) it is possible to determine both Me<sub>3</sub>Al and activator content by integration of these two signals with respect to the total integral due to MAO. The assumption used in our work is that the repeat unit of MAO is (Me<sub>1.5</sub>AlO<sub>0.75</sub>).<sup>[5b]</sup> Alternately, an internal standard may be employed without any assumptions<sup>[5b]</sup> – usually the discrepancy between the two methods is small. Typically,

commercial samples of 30 wt.-% MAO have Me<sub>3</sub>Al content between 13–14 mol-% using this technique while samples of MAO that have been shipped and stored cold have activator contents between 1–2 mol-% when first analyzed by this method.

The positive and negative ion ESI-MS of 10 wt.-% MAO + THF (10 mol-%) are shown in Figure 2a and Figure 2b, respectively. The positive ion spectrum is largely invariant to the amount of THF added (between 1–40 mol-% investigated) with the principle ions present being [Me<sub>2</sub>Al(THF)<sub>2</sub>]<sup>+</sup> and [Me<sub>2</sub>Al(THF)]<sup>+</sup> with *m/z* 201 and 129, respectively. The relative intensity of these two ions is also largely insensitive to the amount of THF added at these levels. At sufficiently low cone voltage (the arbiter of in-source collision energy) only *m/z* 201 is observed.

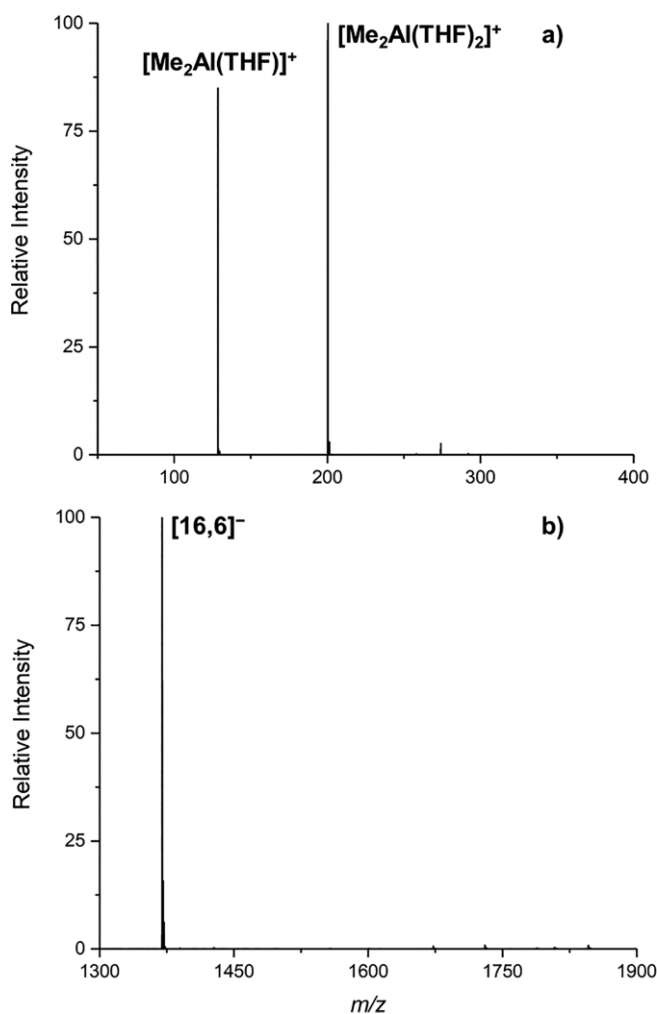


Figure 2. (a) Positive and (b) negative ion mass spectrum of a sample of commercial MAO (10 wt.-% in toluene) containing 10 mol-% THF in PhF solution ([Al] = 0.05 M). Cone voltage = 16 V.

The negative ion mass spectrum resembles that of MAO and other donor additives (vide infra) but at 1–40 mol-% THF the spectra are characterized by a low intensity per transient (<500 counts for the major ion present). The relative intensities of the anions present are insensitive to the amount of THF added, and the mass spectrum is largely dominated by the ion at *m/z* 1375, assigned by *m/z*, isotope pattern and MS/MS behavior as [16,6]<sup>-</sup>.<sup>[10]</sup>

## Octamethyltrisiloxane (OMTS)

Disiloxanes and some cyclic siloxanes have been used as additives to furnish “stabilized MAO”, formulations that are more resistant to gel formation while retaining their activation efficacy.<sup>[18]</sup> With linear, tri- or poly-siloxanes, including OMTS, and at higher concentrations in toluene solution, phase separation occurs to form an upper layer which is enriched in Me<sub>3</sub>Al, and a lower layer that is basically an ionic liquid, swollen by an aromatic solvent<sup>[12]</sup> – first termed a liquid clathrate by Atwood and co-workers based on an ionic host and aromatic guest formalism.<sup>[19]</sup> These liquid clathrates can be isolated in solid form by washing with hydrocarbon solvents, which remove Me<sub>3</sub>Al and toluene.<sup>[12]</sup> <sup>1</sup>H, <sup>27</sup>Al and <sup>29</sup>Si NMR spectra of the solid formed from OMTS have been published in the patent literature in 1,3-dichlorobenzene,<sup>[12]</sup> and the same reaction has been studied in PhF solution.<sup>[7]</sup> These studies strongly indicate that a material with the composition [Me<sub>2</sub>Al(OMTS)]<sup>+</sup>[MAO(Me)]<sup>-</sup> is formed where the composition of the anion was not defined.

In this work, we generated this ion-pair *in situ* in [D<sub>5</sub>]bromobenzene ([D<sub>5</sub>]PhBr) or bromobenzene (PhBr) solution, the intent being to relate the NMR spectra seen to the ESI-MS spectra recorded in PhF solution as the two solvents have similar dielectric constants. Typically, 1–10 mol-% of OMTS was added for this purpose with respect to Al in MAO.

We used two sources of MAO, commercial 30 wt.-% solution as well as a sample of dried MAO prepared from this material for work in deuterated solvents. The 30 wt.-% solution had 13.3 mol-% Me<sub>3</sub>Al and 1.50 mol-% activator content measured using [D<sub>8</sub>]THF as additive, while the dried MAO had a lower Me<sub>3</sub>Al and activator content of 8.3 and 0.94 mol-% by the same technique (see Supporting Information Figure S1).

A <sup>1</sup>H NMR spectrum of the high field region of dried MAO and OMTS appears in Figure 3. Two of the six MeSi signals resolved in this spectrum correspond to free OMTS (**1**) which was added at 7.5 mol-% with respect to Al in solid MAO. A value of 8.1 mol-% was determined from actual integration of all the SiMe signals with respect to the AlMe signals.

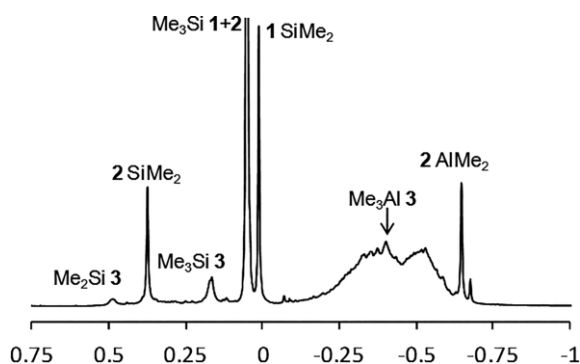
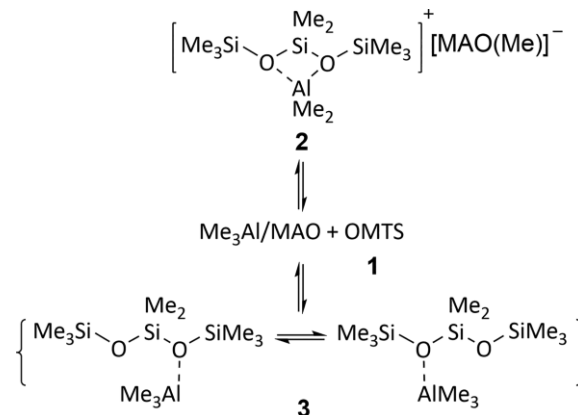


Figure 3. <sup>1</sup>H NMR spectrum of dried MAO and OMTS (7.5 mol-%) in [D<sub>5</sub>]bromobenzene. The most intense signals (SiMe<sub>3</sub> from **1** and **2**) are off-scale and have been cut off.

Two signals due to MeAl groups are present at δ –0.40 and –0.65 ppm in this mixture<sup>[20]</sup> and which show exchange correlation with one another as shown by a selective 1D gradient NOESY spectrum (see Supporting Information Figure S2). The

signal at δ –0.40 ppm appears at the chemical shift position of Me<sub>3</sub>Al in this solvent and is broadened. The sharp signal at –0.65 ppm shows NOE to two of the SiMe signals at δ 0.06 and 0.38 ppm respectively. The integrated ratio of these three signals is 1:3:1 and they are assigned to the [Me<sub>2</sub>Al(OMTS)]<sup>+</sup> cation **2** (Scheme 2), consistent with the reported chemical shifts.<sup>[7]</sup>



Scheme 2. Reaction of OMTS with MAO + Me<sub>3</sub>Al.

In support of this assignment, irradiation of the SiMe<sub>2</sub> signal at δ 0.38 ppm led to exchange correlation with the “free” OMTS SiMe<sub>2</sub> signal at δ 0.01 ppm (the other more intense signal due to free OMTS is at δ 0.05 ppm and is nearly coincident with the SiMe<sub>3</sub> signal of complex **2** at 0.06 ppm) and also to exchange correlation with a line-broadened signal at δ 0.48 ppm. Another line broadened SiMe signal is at δ 0.16 ppm. The two broadened SiMe signals are present in a ratio of 1:3. The broad AlMe signal appears atop the main MAO resonance and its integral value was approximated as 1.5 with respect to the SiMe peaks.

We interpret these results as follows. The major complex present is [Me<sub>2</sub>Al(OMTS)]<sup>+</sup>[**16,6**]<sup>-</sup> which is in equilibrium with both free OMTS and Me<sub>3</sub>Al and/or the Me<sub>3</sub>Al complex(es) thereof. In principle, both mono- and bis-Me<sub>3</sub>Al complexes of OMTS are possible; the relative intensities of the line broadened signals correspond most closely to a fluxional mono-Me<sub>3</sub>Al complex **3** (Scheme 2). The observation of exchange correlations between all species involved implies that ion-pair formation is reversible.

From the intensities of the SiMe signals it can be estimated that the mixture is comprised of [Me<sub>2</sub>Al(OMTS)]<sup>+</sup> (2.4 mol-%), Me<sub>3</sub>Al–OMTS (ca. 0.40 mol-%) and free OMTS (4.7 mol-%) based on the amount of OMTS added to the MAO (7.5 mol-%). From the AlMe signals present, the amount of complex **2** was calculated as 2.7 mol-% and 0.47 mol-% of complex **3** which is in reasonable agreement. However, the total Me<sub>3</sub>Al content calculated from the latter values (3.17 mol-%) is significantly lower than that measured using THF (8.3 + 0.93 = 9.23 mol-%, *vide supra*) suggesting that a significant amount of Me<sub>3</sub>Al (ca. 2/3) is still bound to or incorporated into MAO at OMTS = 7.5 mol-%.

Significantly more activator complex is present at 7.5 mol-% OMTS vs. 10 equiv. of THF (2.7 vs. 0.93 mol-%). In agreement with this finding, the negative ion ESI-MS spectra of MAO + OMTS are more intense at any given ratio as compared with

THF, and the signals due to higher MW anions are proportionately more intense compared to  $m/z$  1375 (cf. Figure 4 with Figure 2b). It should be noted that the amount of OMTS used for ESI-MS (2 mol-%) is lower than that used in the NMR studies (7.5 mol-%). A higher amount was used for the NMR work to facilitate quantitation. In earlier work we showed that as the amount of OMTS was increased (from 1 to 100 mol-%), the higher MW anions became increasingly accentuated relative to  $[16,6]^-$ .<sup>[10]</sup> This suggests that the corresponding neutral precursors are significantly less abundant in MAO than that due to  $[16,6]^-$ , or more likely, are less reactive towards OMTS.

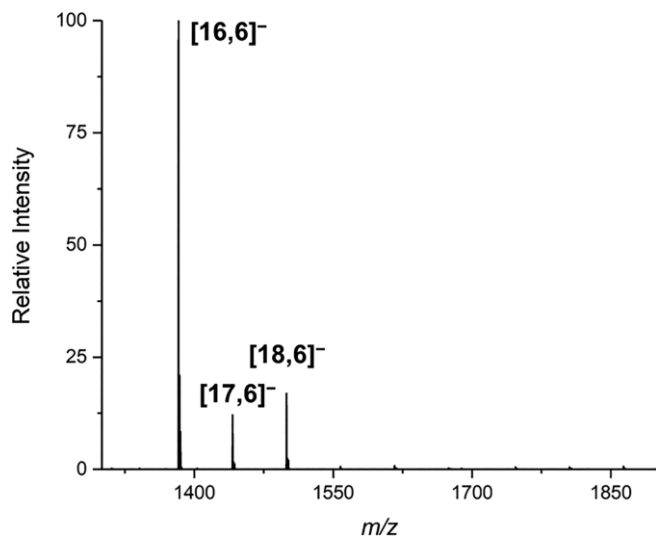
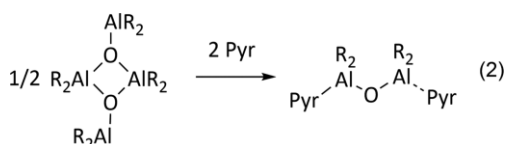


Figure 4. Negative ion mass spectrum of a sample of dried commercial MAO (30 wt-% in toluene) containing 2 mol-% OMTS in PhF solution ( $[Al] = 0.05$  M). Cone voltage = 16 V.

Evidently, a bidentate donor is more effective at abstracting  $[Me_2Al]^+$  from the neutral MAO molecules than a mono-dentate donor of comparably basicity.<sup>[21]</sup> The corresponding positive ion spectrum showed the expected cation with  $m/z$  293.<sup>[10]</sup>

### Pyridine and 2,2'-Bipyridine

Pyridine was originally proposed for determining the  $Me_3Al$  content of MAO but it has since been shown that excess pyridine (>5 equiv.) leads to degradation.<sup>[4b,5b,5c]</sup> Pyridine disrupts dative  $Al \cdots O$  bonding in tetra-*tert*-butyldialuminumoxane, which is dimeric in the solid state and associated in solution, forming a structurally characterized, monomeric bis(pyridine) adduct (Equation 2).<sup>[22]</sup> The mechanism for degradation of MAO by donors is unknown but likely involves similar reactions. We decided to investigate both pyridine, as well as a chelating analogue, to compare with the oxygen-based donors already discussed.<sup>[23]</sup>



Before discussing pyridine, we begin with 2,2'-bipyridine (bipy) which gives well-defined chemistry at low levels with re-

spect to MAO (i.e. < 10 mol-% for the dried MAO). By both NMR and ESI-MS, clean formation of the  $[Me_2Al(bipy)]^+[MAO-Me]^-$  ion-pair is observed.

A  $^1H$  NMR spectrum at 4 mol-% bipy using dried MAO appears in Figure 5, where assignments are based on both COSY and selective 1D NOESY spectra (see Supporting Information Figures S3–S4). Integration of the signals due to bipy vs. MAO +  $Me_3Al$  gave a calculated ratio of 3.4 mol-% suggesting at least 86 % of added bipy forms this complex. At least two sharper  $AlMe$  signals are atop the main broad resonance for MAO. The sharpest signal at  $-0.51$  ppm integrated to roughly 6H with respect to the individual resonances due to bipy (2H each). The other broader signal is again at roughly the chemical shift of  $Me_3Al$  in this solvent (see Figure S5). The total intensity of these two signals corresponded to 5.6 mol-% of total Al with that due to the complex at 3.7 mol-% based on Al. Evidently, almost all of the added bipy forms the complex resulting from  $[Me_2Al]^+$  abstraction, while residual free (ca. 1/3) and bound  $Me_3Al$  (ca. 2/3) comprise the balance of  $Me_3Al$  present.<sup>[4b]</sup>

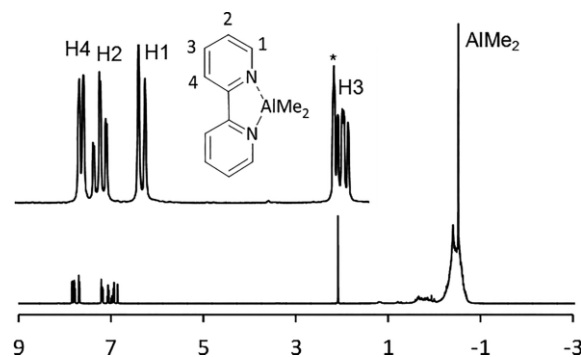


Figure 5.  $^1H$  NMR spectrum of MAO + bipy (4 mol-%) in  $[D_5]PhBr$ . Inset shows expansion of the aromatic region with assignments as indicated. (\* = residual  $C_6D_4HBr$ ).

Bipy forms 1:1 and 1:2 complexes with  $Me_3Al$  that have been characterized.<sup>[24]</sup> A  $^1H$  NMR spectrum of bipy and >2 equiv. of  $Me_3Al$  showed line broadened resonances due to bipy, free and bound  $Me_3Al$  (see Supporting Information Figure S5). These were not observed in the mixture of bipy and MAO suggesting this chelating ligand has a high chemoselectivity for  $[Me_2Al]^+$  abstraction.

Positive and negative ion ESI-MS of MAO and bipy appear in Figure 6. By comparing Figure 6b with Figure 4 and Figure 2b it can be seen that bipy is the most effective donor in forming ion-pairs with the largest range of neutral precursors, based on the relative intensity of the various anions present with respect to  $m/z$  1375. It should be noted that the signal due to  $m/z$  1375 in Figure 6b has saturated the MCP detector (as is evident from the isotope pattern which is distorted compared to the other anions present). In essence of the intensity of the other anions has been accentuated, relative to  $m/z$  1375, by this artefact. Similar effects are also seen with excess OMTS.<sup>[10]</sup> Note that there are also anions lower in MW than  $m/z$  1375 present at this level of bipy. At higher levels of bipy, only lower MW anions were detected in these mixtures (see Supporting Information Figure S6) so that high levels of bipy, like pyridine (or excess OMTS<sup>[10]</sup>) result in degradation of the MAO, presumably

through adduct formation which disrupts dative Al...O bonding as discussed earlier.

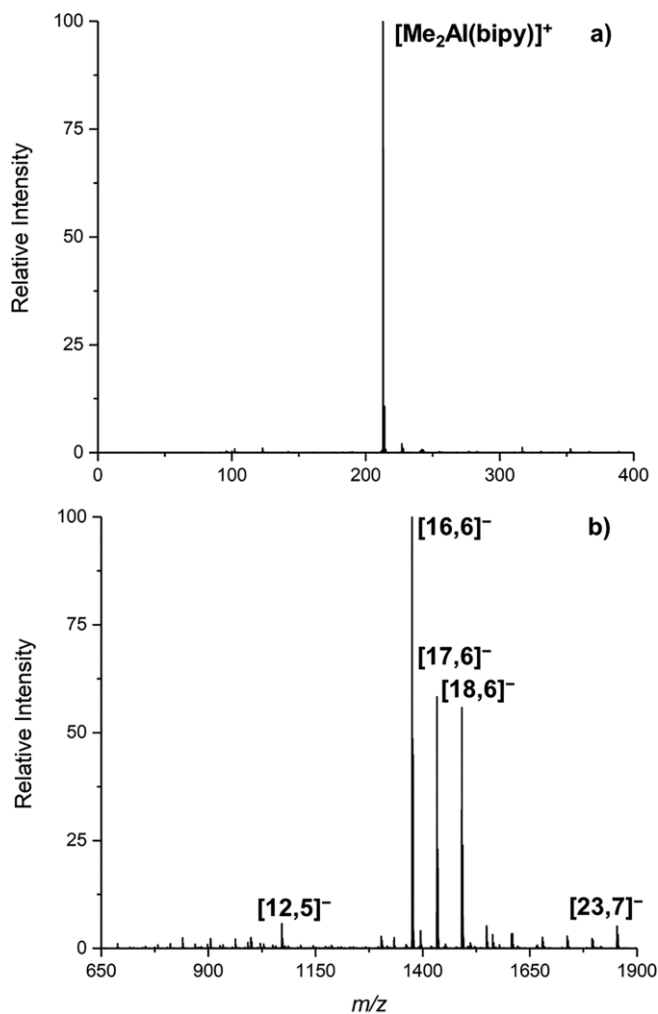


Figure 6. (a) Positive and (b) negative ion ESI-MS spectra of dried MAO + 4 mol-% bipy in  $[D_5]PhBr$  diluted to  $[Al] = 0.02$  M with PhF. Cone voltage = 16 V.

Pyridine shows the most complicated behavior at low levels with respect to MAO.  $^1H$  NMR spectroscopy reveals at least three different complexes are present at the same N loading as bipy (i.e. 8 mol-% Figure 7). The major complexes have line-broadened resonances in the aromatic region. A variable temperature experiment established that the broadening is mainly compositional vs. exchange related (see Supporting Information Figure S7).  $Me_3Al$  forms a known pyridine complex,<sup>[25]</sup> which is present in this spectrum (see Supporting Information Figure S8), but in lowest amounts. The major set of sharp signals at  $\delta$  7.97 (d), 7.55 (t) and 7.17 (dd) ppm are consistent with a  $[Me_2Al(pyr)_2]^+$  cation (see Supporting Information Figures S9–10), which is also detected by ESI-MS (vide infra, Figure 8).

There are three AlMe signals superimposed on the MAO signal at higher field. A sharp signal at  $-0.31$  ppm integrates to ca. 6H with respect to the sharp aromatic signals and is assigned to the AlMe<sub>2</sub> protons of this cation. Selective 1D NOESY experiments support that it is associated with the major set of sharp aromatic signals (see Supporting Information Figure S10). The

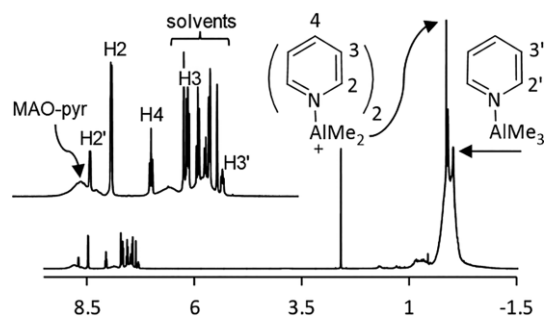


Figure 7.  $^1H$  NMR spectrum of MAO + pyridine (8 mol-%) in  $[D_5]PhBr$ . Inset shows expansion of the aromatic region with assignments.

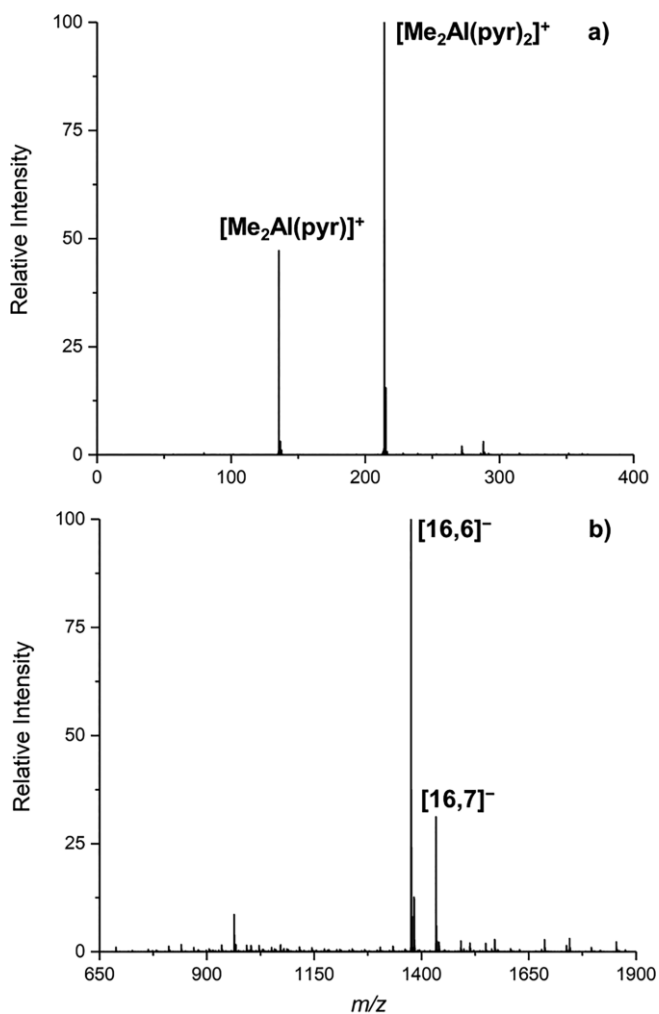


Figure 8. (a) Positive and (b) negative ion MS of dried MAO + 8 mol-% pyridine in  $[D_5]PhBr$  diluted to  $[Al] = 0.02$  M with PhF.

other two signals are broadened and are close to those for  $Me_3Al$  in this solvent ( $-0.4$  ppm) and the corresponding  $Me_3Al$ -pyridine complex (see Supporting Information Figure S8).

If we assign the major broadened, aromatic signals to pyridine adducts with the MAO, then these are present in the amount of 6.3 mol-%, the cation is present at 1.06 mol-%, while the  $Me_3Al$ -pyridine complex is present at 0.58 mol-% based on integration of the aromatic protons. From the integration of the

different MeAl resonances we obtain comparable values of 0.65 and 1.16 mol-% for the neutral Me<sub>3</sub>Al-pyridine and cationic pyridine complexes, with free Me<sub>3</sub>Al accounting for 1.12 mol-% of total aluminoxane. The Me<sub>3</sub>Al content we can account for thus totals 2.98 mol-% which is significantly reduced from that measured using bipy (5.6 mol-%) at the same donor loadings. Based on the total Me<sub>3</sub>Al content measured using THF (i.e. 9.2 mol-%) we cannot account for ca. 2/3 of that so that we expect it is largely associated to the MAO at this low loading of pyridine. Note that much more pyridine is used to measure the Me<sub>3</sub>Al content of MAO<sup>[4b]</sup> than we have used here. It is interesting to note, however, that the activator content measured using this amount of pyridine is quite similar to that measured using excess THF (ca 1 mol-%) in agreement with other work.<sup>[4b]</sup>

The positive and negative ion ESI-MS of pyridine + MAO are shown in Figure 8. As with THF, the appearance of the positive ion MS in Figure 8a is sensitive to cone voltage, suggesting the mono-pyridine complex with *m/z* 136 is derived from fragmentation of the *m/z* 215 ion. In comparing Figure 8b with Figure 6b, it is seen that only [16,6]<sup>-</sup> and [17,6]<sup>-</sup> are especially prominent, while lower MW anions are also present. Thus, the monodentate, and strong donor pyridine shows a different chemoselectivity towards ion-pair formation from MAO compared with bipy, though both additives form lower MW material at the same donor level.

### Theoretical Modeling

In theoretical work, we studied the formation and stability of MAO structures formed by hydrolysis of Me<sub>3</sub>Al.<sup>[16a,16b]</sup> The most stable cage in the real size domain of MAO also has *n* = 16, *m* = 6. The most stable anion [16,6]<sup>-</sup> formed by Me<sup>-</sup> abstraction is shown in Figure 9.

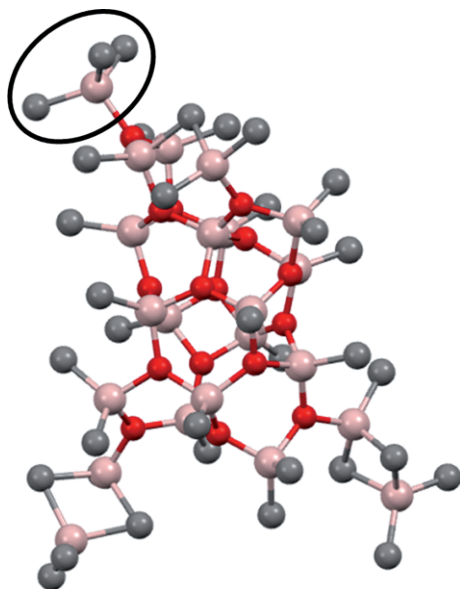


Figure 9. Structure of a model for the [16,6]<sup>-</sup> anion with H-atoms omitted for clarity. The site where Me<sup>-</sup> abstraction has occurred is circled.

Shown in Table 1 are the relative stabilities of neutral cages with *n* = 16–18 for values of *m* corresponding to energy min-

ima. Through the use of the Boltzmann distribution and the actual differences in free energy ( $\Delta(\Delta_r G) \times n$ ), the mole fractions of each neutral (*x<sub>i</sub>*) were calculated. It can be seen the neutrals **16,5** and **16,6** have comparable stability, and comprise about 3/4 of the mixture, while neutrals with *n* = 18, and *m* = 4–6 are present at ca. 15 % abundance, and *n* = 17 with *m* = 4–6 comprising the balance with ca. 10 mol-%.

Table 1. Relative stabilities of (MeAlO)<sub>*n*</sub>(Me<sub>3</sub>Al)<sub>*m*</sub>, where *n* = 16–18, calculated by the M06-2X/TZVP method.

<i>n</i>	<i>m</i>	Formula	$\Delta(\Delta_r G)^{[a]}$	$\Delta(\Delta_r G) \times n$	<i>x<sub>i</sub></i>
16	0	Me <sub>16</sub> Al <sub>16</sub> O <sub>16</sub>	0.1	1.6	0.000
16	1	Me <sub>19</sub> Al <sub>17</sub> O <sub>16</sub>	-1.4	-22.4	0.000
16	2	Me <sub>22</sub> Al <sub>18</sub> O <sub>16</sub>	-4.9	-78.4	0.000
16	3	Me <sub>25</sub> Al <sub>19</sub> O <sub>16</sub>	-5.4	-86.4	0.000
16	4	Me <sub>28</sub> Al <sub>20</sub> O <sub>16</sub>	-5.5	-88.0	0.000
<b>16</b>	<b>5</b>	<b>Me<sub>31</sub>Al<sub>21</sub>O<sub>16</sub></b>	<b>-7.4</b>	<b>-118.4</b>	<b>0.256</b>
<b>16</b>	<b>6</b>	<b>Me<sub>34</sub>Al<sub>22</sub>O<sub>16</sub></b>	<b>-7.5</b>	<b>-120.0</b>	<b>0.489</b>
16	7	Me <sub>37</sub> Al <sub>23</sub> O <sub>16</sub>	-3.7	-59.2	0.000
17	0	Me <sub>17</sub> Al <sub>17</sub> O <sub>17</sub>	4.0	68	0.000
17	1	Me <sub>20</sub> Al <sub>18</sub> O <sub>17</sub>	-1.9	-32.3	0.000
17	2	Me <sub>23</sub> Al <sub>19</sub> O <sub>17</sub>	-4.5	-76.5	0.000
17	3	Me <sub>26</sub> Al <sub>20</sub> O <sub>17</sub>	-4.6	-78.2	0.000
<b>17</b>	<b>4</b>	<b>Me<sub>29</sub>Al<sub>21</sub>O<sub>17</sub></b>	<b>-6.4</b>	<b>-108.8</b>	<b>0.005</b>
<b>17</b>	<b>5</b>	<b>Me<sub>32</sub>Al<sub>22</sub>O<sub>17</sub></b>	<b>-6.5</b>	<b>-110.5</b>	<b>0.011</b>
<b>17</b>	<b>6</b>	<b>Me<sub>35</sub>Al<sub>23</sub>O<sub>17</sub></b>	<b>-6.8</b>	<b>-115.6</b>	<b>0.083</b>
17	7	Me <sub>38</sub> Al <sub>24</sub> O <sub>17</sub>	-3.9	-66.3	0.000
18	0	Me <sub>18</sub> Al <sub>18</sub> O <sub>18</sub>	3.5	63	0.000
18	1	Me <sub>21</sub> Al <sub>19</sub> O <sub>18</sub>	-2.2	-39.6	0.000
18	2	Me <sub>24</sub> Al <sub>20</sub> O <sub>18</sub>	-4.2	-75.6	0.000
18	3	Me <sub>27</sub> Al <sub>21</sub> O <sub>18</sub>	-5.3	-95.4	0.000
<b>18</b>	<b>4</b>	<b>Me<sub>30</sub>Al<sub>22</sub>O<sub>18</sub></b>	<b>-6.1</b>	<b>-109.8</b>	<b>0.008</b>
<b>18</b>	<b>5</b>	<b>Me<sub>33</sub>Al<sub>23</sub>O<sub>18</sub></b>	<b>-5.9</b>	<b>-106.2</b>	<b>0.002</b>
<b>18</b>	<b>6</b>	<b>Me<sub>36</sub>Al<sub>24</sub>O<sub>18</sub></b>	<b>-6.5</b>	<b>-117</b>	<b>0.146</b>
18	7	Me <sub>39</sub> Al <sub>25</sub> O <sub>18</sub>	-4.4	-79.2	0.000

[a]  $\Delta(\Delta_r G)$  (kJ mol<sup>-1</sup> n<sup>-1</sup>) is for the reaction of (*n*+*m*) Me<sub>3</sub>Al + *n* H<sub>2</sub>O → (MeAlO)<sub>*n*</sub>(Me<sub>3</sub>Al)<sub>*m*</sub> + 2*n* CH<sub>4</sub> and are referenced to that energy for the aluminoxane with *n,m* = 4,4.<sup>[16]</sup>

While this is in qualitative agreement with relative anion intensities seen using chelating bases (e.g. Figure 4 and Figure 6), it should be recognized that *none* of these neutrals could form an anion with *m* = 6 by the process of [Me<sub>2</sub>Al]<sup>+</sup> abstraction, as none of them have the correct value of *m* = 7.

In fact, for *n* = 16–18, the structures with *m* = 7 are 40–60 kJ mol<sup>-1</sup> higher in energy than the most stable structures (Table 1). Moreover, anionization potentials  $\Delta G_{AP}$  for [Me<sub>2</sub>Al]<sup>+</sup> abstraction predict that **17,7** and **18,7** should be more reactive species for this process ( $\Delta\Delta G_{AP}$  16–48 kJ mol<sup>-1</sup> with respect to **16,7** Table 2, entries 4–6) while **18,6** is the most reactive towards Me<sup>-</sup> abstraction (by ca. 35 kJ mol<sup>-1</sup>, Table 2).

One can calculate from  $\Delta G_{AP}$  and the population of each precursor (Table 1) a theoretical intensity distribution. This can be compared to an experimental distribution, which we admit is donor dependent, such as [16,6]<sup>-</sup> (77.4 ± 1.2 %), [17,6]<sup>-</sup> (2.1 %) and [18,6]<sup>-</sup> (9.9 %) at 100:1 Al:OMTS (see Supporting Information Figure S12). The only distribution which is even close to this experimental distribution involves [Me<sub>2</sub>Al]<sup>+</sup> abstraction from the **n,6** precursors (entries 1–3 Table 2) which should form [**n,5**]<sup>-</sup> anions vs. [**n,6**]<sup>-</sup> which are observed.

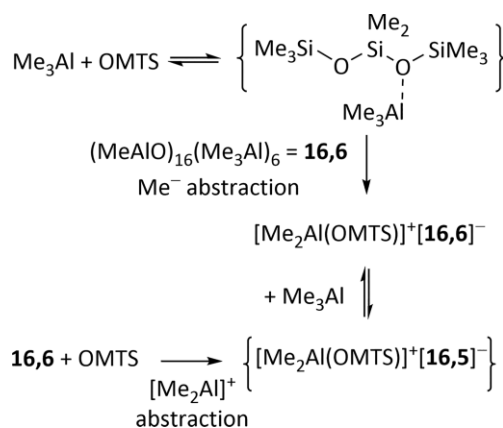
There are several plausible explanations of why a discrepancy exists between theory vs. experiment for ionization involv-

Table 2. Anionization potentials  $\Delta G_{AP}$  for neutral aluminoxanes with  $n = 16$ –18 and  $m = 6$ –7.

Entry	$n$	$m$	$\Delta G_{AP} \text{ Me}_2\text{Al}^+$	$w_{X_i}^{[a]}$	$\Delta G_{AP} \text{ Me}^-$	$w_{X_i}^{[a]}$
1	16	6	-144.6	0.584 [16,5]	-125.8	0.000 [16,6]
2	17	6	-148.3	0.009 [17,5]	-142.5	0.004 [17,6]
3	18	6	-159.7	0.406 [18,5]	-160.8	0.995 [18,6]
4	16	7	-143.7	0.000 [16,6]	-	-
5	17	7	-191.7	0.999 [17,6]	-	-
6	18	7	-159.5	0.000 [18,6]	-	-

[a]  $w_{X_i}$  is the theoretical anion intensity distribution, calculated using the Boltzmann distribution using  $\Delta G_{AP}$  and weighted by the population of the corresponding neutral precursor (see Table 1).

ing neutral donors without ionizable methyl groups: 1) The neutral MAO molecules located by theory do not correspond to the species undergoing ionization, or their relative stability/reactivity is poorly estimated. 2) The donors studied bind reversibly to  $\text{Me}_3\text{Al}$  which is abundant in MAO solutions, and it is the resulting adduct(s) which are reactive to ionization by the process of  $\text{Me}^-$  abstraction (Scheme 3, top) and/or 3) ionization does involve  $\text{Me}_2\text{Al}^+$  abstraction from **16,6** but the resulting anion **[16,5]**<sup>-</sup> binds  $\text{Me}_3\text{Al}$  strongly such that we detect only the observed anion **[16,6]**<sup>-</sup> (Scheme 3, bottom).



Scheme 3. Alternative mechanisms for ion-pair formation.

We admit that the first possibility is entirely real. For molecules of this size, the number of isomers is enormous and there is no guarantee that our grid search has located the global minimum. ESI-MS does not detect the most stable neutrals present, only those which can readily ionize – it is possible that an isomer of **16,6** that is highly reactive towards  $[\text{Me}_2\text{Al}]^+$  abstraction is significantly higher in energy than the structure we located (and by inference, all the other precursor structures too). Also, relative ion intensities in ESI-MS do not track relative concentrations exactly, even where the ions in question are structurally similar to each other. Finally, calculated  $\Delta G_{AP}$  neglect ion-pairing or donor strengths which will be important in condensed phase and in solvents like PhF which are moderately polar. Thus, we should not be too surprised that our calculated intensity distributions do not reproduce experimental results.

The second explanation (Scheme 3, top) is interesting in the sense that the observed anion distributions are not very sensitive to donor base strength. Compare e.g. Figure 6b with 4

where the base strength of bipy and OMTS differs by about six orders of magnitude.<sup>[21]</sup> This does not make much sense unless the base strength of these donors has been leveled, e.g. by prior binding to  $\text{Me}_3\text{Al}$ .

In fact, bipy (or OMTS<sup>[10]</sup>) and excess  $\text{Me}_3\text{Al}$  can be reacted with one another to form these adducts and then added to MAO; the resulting ESI-MS spectra are very similar to those observed on direct addition at the same additive level (see Supporting Information Figure S11).

Calculations show that reaction of a THF- $\text{AlMe}_3$  adduct with **16,6** by  $\text{Me}^-$  abstraction will be favored over  $[\text{Me}_2\text{Al}]^+$  abstraction from **16,7** by 40–50  $\text{kJ mol}^{-1}$  (Figure 10). In this case, the structure of the resulting anions is different with the former process leading to the most stable anion (Figure 9). However, DFT calculations on an assembly of **16,6** with an  $\text{Al-Me}$  bond of THF- $\text{AlMe}_3$  in close proximity to a site with the highest latent Lewis acidity – i.e. a strained, tetrahedral  $(\mu\text{-O})\text{Me}_2\text{Al}\cdots\text{MeAl}(\text{Me})(\mu\text{-O})$  site, failed to produce a stationary point with significant  $\text{Al-C}$  bond cleavage or formation (see Supporting Information). Thus, there may be a kinetic barrier to  $\text{Me}^-$  abstraction by this mechanism.

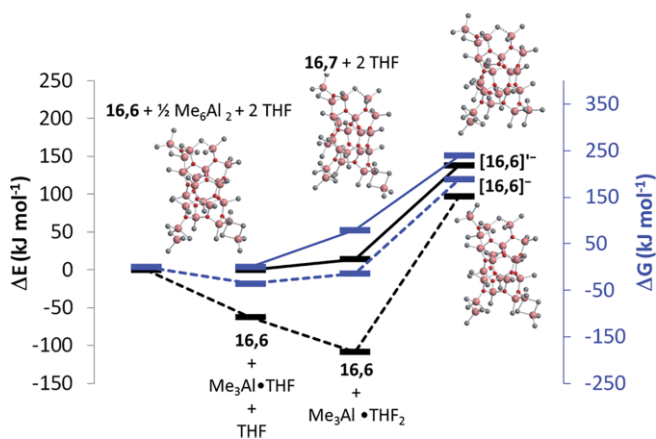


Figure 10. Calculated energy and free differences for ionization by  $\text{Me}^-$  abstraction (bottom dashed pathways) vs.  $[\text{Me}_2\text{Al}]^+$  abstraction (top solid pathways) involving **16,6** and  $\text{Me}_3\text{Al} + 2 \text{ THF}$ . Free energy differences are in blue, while energy differences are in black.

On the other hand, chelated ion pairs are directly formed from bipy, and either **16,7** or **16,6** by  $[\text{Me}_2\text{Al}]^+$  abstraction from either basal  $\text{Al}_2\text{Me}_5$  site (Figure 11). In the case of **16,6** the processes are exergonic by about 39–42  $\text{kJ mol}^{-1}$  leading to contact ion-pairs. Reaction of **16,7** at these two sites is exergonic by 45–78  $\text{kJ mol}^{-1}$  suggesting **16,7** will be the more reactive precursor. However, the higher reactivity of this precursor ( $\Delta\Delta G \leq -36 \text{ kJ mol}^{-1}$ ) will be entirely offset by its lower stability ( $\Delta\Delta G = 60.8 \text{ kJ mol}^{-1}$  Table 1). In essence, **16,7** will contribute about 60 ppm towards ionization by this mechanism, as estimated using the van't Hoff equation with  $\Delta\Delta G = 60.8 + 42 - 78 \text{ kJ mol}^{-1} = 24.8 \text{ kJ mol}^{-1}$ .

On this basis, the 3<sup>rd</sup> explanation (Scheme 3) can also not be excluded. Anion **[16,6]**<sup>-</sup> is prone to loss of two  $\text{Me}_3\text{Al}$  moieties at lowest collision energies during MS/MS experiments, and 1–2 losses at higher cone voltages, certainly suggesting that the 1<sup>st</sup>  $\text{Me}_3\text{Al}$  is reversibly bound. In Figure 12 the break down

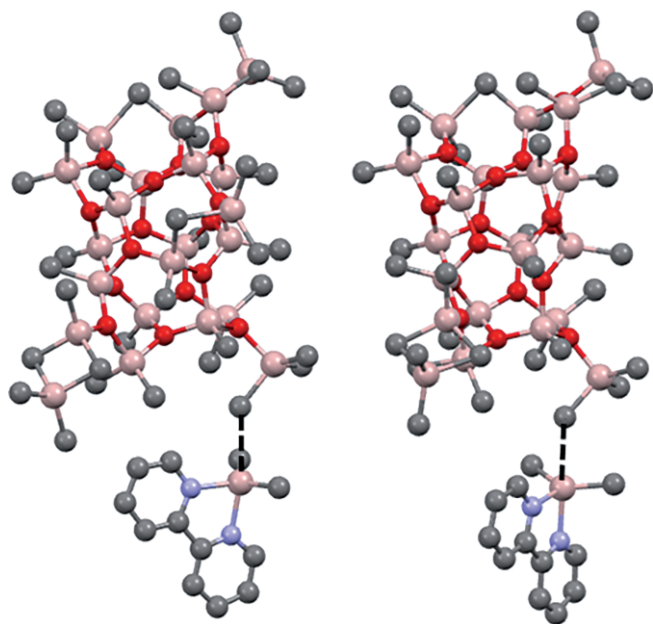


Figure 11. Chelated ion-pairs formed from **16,7** (left) and **16,6** (right) + bipy. The shortest contacts between anion and cation are shown with a dashed line with distances of 3.13 and 3.08 Å, respectively.

curve for  $[\mathbf{16,6}]^-$  vs. the mass-corrected collision energy is shown, where the first loss of  $\text{Me}_3\text{Al}$  is about 50 % complete at  $E_0 = 0.37$  V.

$$E_0(\text{V}) = \frac{m_{\text{Ar}}}{m_{\text{Ar}} + m_{[\mathbf{16,6}]}} \times E_{\text{lab}}$$

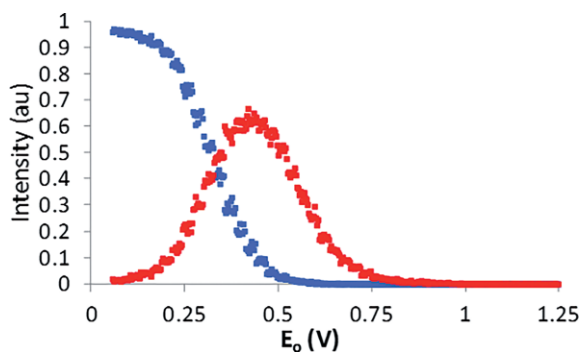


Figure 12. Break-down curve for CID of  $\text{Me}_3\text{Al}$  from the anion  $[\mathbf{16,6}]^-$  vs. mass-corrected, collision energy.

That number, in and of itself, is not meaningful but it happens to be identical in magnitude to that observed for collision-induced dissociation (CID) of  $\text{Me}_3\text{Al}$  from the ion  $[\text{Cp}_2\text{ZrMe}_2\text{AlMe}_2]^+$  using He as the collision gas under otherwise identical conditions (see Supporting Information Figure S13). This suggests that the binding of  $\text{Me}_3\text{Al}$  to the  $[\mathbf{16,5}]^-$  anion is certainly of comparable strength to the binding of  $\text{Me}_3\text{Al}$  to  $[\text{Cp}_2\text{ZrMe}]^+$  for which the equilibrium constant is known ( $K = 2.12 \times 10^3 \text{ M}^{-1}$  at 40 °C in benzene).<sup>[26]</sup> Thus, we certainly cannot exclude the possibility that donors react directly with precursors like **16,6** furnishing  $[\mathbf{16,5}]^-$  which rapidly scavenges free  $\text{Me}_3\text{Al}$  to give  $[\mathbf{16,6}]^-$ .

## Conclusions

ESI-MS is a very useful adjunct to the arsenal of spectroscopic methods for characterization of MAO. However, these initial studies have provoked as many mechanistic questions as they address, especially as to the structure of MAO and fundamental mechanisms for ion-pair formation. The results can be interpreted in terms of  $\text{Me}^-$  abstraction from a  $\text{Me}_3\text{Al}$  adduct by the most reactive MAO precursors, or alternately direct  $[\text{Me}_2\text{Al}]^+$  abstraction from the most stable precursor by the donor, followed by binding of  $\text{Me}_3\text{Al}$  to the resulting anion. It is quite conceivable, based on the interplay between  $\text{Me}_3\text{Al}$  content vs. donor amount and strength that more than one mechanism is operative depending on neutral MAO precursor. Finally, it is evident from this paper that the  $\text{Me}_3\text{Al}$  and activator content of MAO appear donor dependent at the levels studied. Strong bidentate donors react completely with the available precursors (and  $\text{Me}_3\text{Al}$ ) to furnish ion-pairs vs. a more nuanced competition between ionization and adduct formation with  $\text{Me}_3\text{Al}$  (or MAO) in the case of mono-dentate bases. It will be interesting to examine whether different metallocenium ion precursors show similar chemoselectivity, leading to different amounts of ion-pairs as well as a common cation partnered with different anions.

## Experimental Section

**Purification of Reagents:** Pyridine (Sigma Aldrich), fluorobenzene (Oakwood), bromobenzene (Sigma Aldrich) and  $[\text{D}_6]$ bromobenzene (Cambridge Isotopes) were all distilled from  $\text{CaH}_2$  under  $\text{N}_2$  and stored over activated 4Å molecular sieves (20 % w/v) for several days prior to use. Tetrahydrofuran (Sigma Aldrich) or  $[\text{D}_8]$ tetrahydrofuran (Cambridge Isotopes) was purified by passage through activated alumina under  $\text{N}_2$  and stored over activated sieves for several days prior to use. 2,2'-Bipyridine (Sigma Aldrich) was used as received but stored in a glove-box as it is hygroscopic. Octamethyltrisiloxane (Sigma Aldrich) was used as received and stored in a glove-box prior to use.

**NMR Experiments:** 1D and 2D  $^1\text{H}$  NMR experiments were conducted in  $[\text{D}_5]$ bromobenzene ( $[\text{D}_5]$ PhBr) solution so as to mimic the ESI-MS experiments in PhF solution. These two solvents have similar dielectric constants, though  $[\text{D}_5]$ PhBr is a softer donor than PhF. Selective 1D and 2D NMR experiments involved use of an inverse detection probe-head and were conducted at 500 MHz using a Bruker instrument. Variable temperature NMR experiments were conducted at 360 MHz using a normal detection probe-head calibrated using MeOH and a Bruker spectrometer using undeuterated solvents and added  $[\text{D}_6]$ benzene for lock. Chemical shifts are referenced with respect residual lock solvent.

**ESI-MS Experiments:** In a typical procedure, a stock solution (ca. 3 mL) was prepared from MAO (0.75 mL of ca. 1.0 M) and the amount of a PhF solution of OMTS (0.5 mL of 0.015 M) needed to give an Al:OMTS ratio of ca. 100:1. After mixing, the stock solution was further diluted with PhF so as to provide a final solution ca. 1.5 mM in Al. The same procedure was used to obtain the THF, pyridine, and 2,2'-bipyridine mixtures. This solution was analyzed using a Micromass QTOF *micro* mass spectrometer via pumping it at ca. 40  $\mu\text{L}/\text{min}$  through PTFE tubing (1/16" o.d., 0.005" i.d.) to the ESI-MS probe and source using a syringe pump. Capillary voltage



was set at 2700 V with source and desolvation gas temperature at 85 °C and 185 °C, respectively with the desolvation gas flow at 400 L/h. MS/MS data were obtained on product ion spectra using argon as the collision gas and a voltage range of 2–100 V.

**Computational Details:** Models for the neutral MAOs were produced by following the Me<sub>3</sub>Al hydrolysis reactions, precisely by the procedure reported previously.<sup>[16a,16b]</sup> Association of Me<sub>3</sub>Al into the MAO oligomers gives rise to dispersive interactions that complicate theoretical treatment of these molecules.<sup>[27]</sup> The M06 series of functionals<sup>[28]</sup> has been recently shown as a cost-effective alternative for correlated ab initio methods in studies involving MAO.<sup>[27,29]</sup> The calculations were carried out at M062X/TZVP level of theory<sup>[30]</sup> using Gaussian 09.<sup>[31]</sup> Stationary points were confirmed as true local minima in the potential energy surface by calculation of harmonic vibrational frequencies. Free energy values have been corrected by a factor of 2/3ΔS as recommended for condensed phase.<sup>[32]</sup>

The feasibility of anion formation via [Me<sub>2</sub>Al]<sup>+</sup> loss from a neutral MAO was based on the relative anionization potential, which is determined from the energy of the reaction MAO → [Me<sub>2</sub>Al]<sup>+</sup> [MAO-Me]<sup>-</sup>.<sup>[9]</sup> The feasibility of anion formation via Me-abstraction was based on the energy of the reaction MAO + Me<sup>-</sup> → [MAO-Me]<sup>-</sup>.<sup>[9]</sup> Both ionization energies are given relative to those for trimethylaluminum dimer.<sup>[9]</sup>

#### Author Information

The authors declare no competing financial interest.

#### Acknowledgments

We thank NOVA Chemicals' Centre for Applied Research for financial support. We thank Albemarle Corp. for a kind donation of MAO, and Dr. Bill Beard for helpful discussions. J. S. M. thanks NSERC (Strategic Project Grant #478998-15) for operational funding and CFI, BCKDF, and the University of Victoria for infrastructural support. S. C. acknowledges support for a Visiting Scientist position from the University of Victoria and the assistance of Dr. Christopher Barr with the NMR experiments performed. M. L. acknowledges grants from the 7<sup>th</sup> Framework Programme of the European Commission (246274), the Academy of Finland (251448) and of computer capacity from the Finnish Grid & Cloud Infrastructure (urn:nbn:fi:research-infras-2016072533).

**Keywords:** Methylaluminoxane · Activators · Cocatalysts · Donor-acceptor systems · Homogeneous catalysis · Density functional calculations

- [1] a) H. S. Zijlstra, S. Harder, *Eur. J. Inorg. Chem.* **2015**, 2015, 19–43; b) M. Bochmann, *Organometallics* **2010**, 29, 4711–4740; c) E. Y.-X. Chen, T. J. Marks, *Chem. Rev.* **2000**, 100, 1391–1434.
- [2] W. Kaminsky, *Macromolecules* **2012**, 45, 3289–3297.
- [3] D. B. Malpass, in *Handbook of Transition Metal Polymerization Catalysts* (Eds.: R. Hoff, R. T. Mathers), John Wiley & Sons, Hoboken, NJ, **2010**, pp. 1–28.
- [4] a) H. S. Zijlstra, M. C. A. Stuart, S. Harder, *Macromolecules* **2015**, 48, 5116–5119; b) F. Ghiotto, C. Pateraki, J. Tanskanen, J. R. Severn, N. Luehmann, A. Kusmin, J. Stellbrink, M. Linnolahti, M. Bochmann, *Organometallics* **2013**, 32, 3354–3362; c) L. Rocchigiani, V. Busico, A. Pastore, A. Macchioni, *Dalton Trans.* **2013**, 42, 9104–9111; d) J. Stellbrink, A. Niu, J. Allgaier, D. Richter, B. W. Koenig, R. Hartmann, G. W. Coates, L. J. Fetters, *Macromolecules* **2007**, 40, 4972–4981; e) D. E. Babushkin, H.-H. Brintzinger, *J. Am. Chem. Soc.* **2002**, 124, 12869–12873; f) E. W. Hansen, R. Blom, P. O. Kvernberg, *Macromol. Chem. Phys.* **2001**, 202, 2880–2889.
- [5] a) D. W. Imhoff, L. S. Simeral, D. R. Blevins, W. R. Beard, *ACS Symp., Ser.* **1999**, 749, 177–191 and references cited therein; b) D. W. Imhoff, L. S. Simeral, S. A. Sangokoya, J. H. Peel, *Organometallics* **1998**, 17, 1941–1945; c) A. R. Barron, *Organometallics* **1995**, 14, 3581–3583.
- [6] See e.g a) C. Ehm, R. Cipullo, P. H. M. Budzelaar, V. Busico, *Dalton Trans.* **2016**, 45, 6847–6855; b) V. Busico, R. Cipullo, R. Pellecchia, G. Talarico, A. Razavi, *Macromolecules* **2009**, 42, 1789–1791 and references cited therein.
- [7] L. Luo, S. A. Sangokoya, X. Wu, S. P. Diefenbach, B. Kneale, *US Patent 8,575,284* **2013**, 18 pp.
- [8] T. K. Trefz, M. A. Henderson, M. Y. Wang, S. Collins, J. S. McIndoe, *Organometallics* **2013**, 32, 3149–3152.
- [9] a) J. T. Hirvi, M. Bochmann, J. R. Severn, M. Linnolahti, *ChemPhysChem* **2014**, 15, 2732–2742; b) M. S. Kuklin, J. T. Hirvi, M. Bochmann, M. Linnolahti, *Organometallics* **2015**, 34, 3586–3597.
- [10] H. S. Zijlstra, M. Linnolahti, S. Collins, J. S. McIndoe, *Organometallics* **2017**, 36, 1803–1809.
- [11] T. K. Trefz, M. A. Henderson, M. Linnolahti, S. Collins, J. S. McIndoe, *Chem. Eur. J.* **2015**, 21, 2980–2991.
- [12] S. A. Sangokoya, B. L. Goodall, L. S. Simeral, *Int. Pat WO 2003/082879*, **2003**, 54 pp.
- [13] S. Collins, M. Linnolahti, M. G. Zamora, H. S. Zijlstra, M. T. R. Hernández, O. Perez-Camacho, *Macromolecules* **2017**, 50, 8871–8884.
- [14] H. S. Zijlstra, S. Collins, J. S. McIndoe, *Chem. Eur. J.* **2018**, 24, 5506–5512.
- [15] H. S. Zijlstra, A. Joshi, M. Linnolahti, S. Collins, J. S. McIndoe, *Dalton Trans.* **2018**, 47, 17291–17298.
- [16] a) M. Linnolahti, S. Collins, *ChemPhysChem* **2017**, 18, 3369–3374; b) M. Linnolahti, A. Laine, T. A. Pakkanen, *Chem. Eur. J.* **2013**, 19, 7133; c) Z. Falls, N. Tyimińska, E. Zurek, *Macromolecules* **2014**, 47, 8556–8569; d) E. Zurek, T. K. Woo, T. K. Firman, T. Ziegler, *Inorg. Chem.* **2001**, 40, 361–370; e) E. Zurek, T. Ziegler, *Inorg. Chem.* **2001**, 40, 3279–3292.
- [17] A. F. R. Kilpatrick, J.-C. Buffet, P. Norby, N. H. Rees, N. P. Funnell, S. Sripathongnak, D. O'Hare, *Chem. Mater.* **2016**, 28, 7444–7450.
- [18] S. A. Sangokoya, *U. S. Patent 5,731,253* **1998**, 10 pp.
- [19] L. R. MacGillivray, J. L. Atwood, *Angew. Chem. Int. Ed.* **1999**, 38, 1018–1033; *Angew. Chem.* **1999**, 111, 1080 and references cited therein.
- [20] There is an additional minor signal at high field that corresponds to oxidized Me<sub>3</sub>Al – i.e. (Me<sub>2</sub>AlOMe)<sub>n</sub> with signals due to OMe seen between 3–4 ppm.
- [21] B. D. Shepherd, *J. Am. Chem. Soc.* **1991**, 113, 5581–5583 and references cited therein.
- [22] M. R. Mason, J. M. Smith, S. G. Bott, A. R. Barron, *J. Am. Chem. Soc.* **1993**, 115, 4971–4984.
- [23] We note that various phosphine donors and MAO have been studied by both Barron and co-workers (ref. 5c) as well as Bochmann and co-workers (ref. 4). In agreement with their results we detect no signals due to a [Me<sub>2</sub>Al(PPh<sub>3</sub>)<sub>n</sub>]<sup>+</sup> cation by positive ion ESI-MS in PhF solution.
- [24] S. Hasenzahl, W. Kaim, T. Stahl, *Inorg. Chim. Acta* **1994**, 225, 23–34 and references cited therein.
- [25] B. Wrackmeyer, E. V. Klimkina, W. Milius, *Eur. J. Inorg. Chem.* **2009**, 2009, 3163–3171 and references cited therein.
- [26] J. M. Camara, R. A. Petros, J. R. Norton, *J. Am. Chem. Soc.* **2011**, 133, 5263–5273.
- [27] Ehm, G. Antinucci, P. H. M. Budzelaar, V. Busico, *J. Organomet. Chem.* **2014**, 772–773, 161–171.
- [28] Y. Zhao, D. G. Truhlar, *Theor. Chem. Acc.* **2008**, 120, 215–241.
- [29] Z. Boudene, T. De Bruin, H. Toulhoat, P. Raybaud, *Organometallics* **2012**, 31, 8312–8322.
- [30] A. Schäfer, C. Huber, R. Ahlrichs, *J. Chem. Phys.* **1994**, 100, 5829–5835.
- [31] M. J. Frisch, G. W. Trucks, H. B. Schlegel, G. E. Scuseria, M. A. Robb, J. R. Cheeseman, G. Scalmani, V. Barone, B. Mennucci, G. A. Petersson, H. Nakatsuji, M. Caricato, X. Li, H. P. Hratchian, A. F. Izmaylov, J. Bloino, G. Zheng, J. L. Sonnenberg, M. Hada, M. Ehara, K. Toyota, R. Fukuda, J. Hasegawa, M. Ishida, T. Nakajima, Y. Honda, O. Kitao, H. Nakai, T. Vreven, J. A. Montgomery Jr., J. E. Peralta, F. Ogliaro, M. Bearpark, J. J. Heyd, E. Brothers, K. N. Kudin, V. N. Staroverov, R. Kobayashi, J. Normand, K. Raghava-

chari, A. Rendell, J. C. Burant, S. S. Iyengar, J. Tomasi, M. Cossi, N. Rega, J. M. Millam, M. Klene, J. E. Knox, J. B. Cross, V. Bakken, C. Adamo, J. Jaramillo, R. Gomperts, R. E. Stratmann, O. Yazyev, A. J. Austin, R. Cammi, C. Pomelli, J. W. Ochterski, R. L. Martin, K. Morokuma, V. G. Zakrzewski, G. A. Voth, P. Salvador, J. J. Dannenberg, S. Dapprich, A. D. Daniels, Ö. Farkas, J. B. Foresman, J. V. Ortiz, J. Cioslowski, D. J. Fox, Gaussian 09, Revision C.01, Gaussian, Inc., Wallingford CT, 2010.

[32] a) S. Tobisch, T. Ziegler, *J. Am. Chem. Soc.* **2004**, *126*, 9059–9071; b) F. Zaccaria, C. Ehm, P. H. M. Budzelaar, V. Busico, *ACS Catal.* **2017**, *7*, 1512; c) F. Zaccaria, R. Cipullo, P. H. M. Budzelaar, V. Busico, C. Ehm, *J. Polym. Sci., Part A J. Polym. Sci., Part A: Polym. Chem.* **2017**, *55*, 2807.

---

Received: February 8, 2019